



# MicroRNA-186-5p inhibits H9c2 cells apoptosis induced by oxygen-glucose deprivation by targeting ERK1/2

Wennan Nie<sup>1#</sup>, Jia Wu<sup>1#</sup>, Xiaoyang Yu<sup>1,2#</sup>, Zhuolin Li<sup>1</sup>, Xiaomin Cai<sup>3</sup>, Wenyan Wei<sup>1</sup>, Cheng Wang<sup>1</sup>, Junjun Wang<sup>1</sup>

<sup>1</sup>Department of Clinical Laboratory, Jinling Hospital, Medical School of Nanjing University, Nanjing, China; <sup>2</sup>School of Medicine, Jiangsu University, Zhenjiang, China; <sup>3</sup>Department of Cardiology, Jinling Hospital, Medical School of Nanjing University, Nanjing, China

**Contributions:** (I) Conception and design: W Nie, J Wu, J Wang; (II) Administrative support: J Wang; (III) Provision of study materials or patients: W Nie, J Wu, X Yu; (IV) Collection and assembly of data: W Nie, J Wu, X Yu; (V) Data analysis and interpretation: W Nie, J Wu, X Yu; (VI) Manuscript writing: All authors; (VII) Final approval of manuscript: All authors.

<sup>#</sup>These authors contributed equally to this work.

**Correspondence to:** Junjun Wang, Department of Clinical Laboratory, Jinling Hospital, Medical School of Nanjing University, 305 East Zhongshan Road, Nanjing 210002, China. Email: wangjunjun9202@163.com.

**Background:** Serum miR-186-5p levels are increased in acute myocardial infarction (AMI) patients and might contribute to assessing the prognosis of AMI patients. In this study, we further investigated the underlying molecular mechanism of miR-186-5p that participated in the pathological processes of myocardial ischemia.

**Methods:** The AMI models of rats and oxygen-glucose deprivation (OGD) models of H9c2 cells were established. Bioinformatics databases, luciferase reporting, and western blotting assays were performed to identify the regulatory target of miR-186-5p. Transfection and functional experiments were conducted to further define the possible molecular mechanism of miR-186-5p during the process of glucose deficiency and hypoxia.

**Results:** The level of miR-186-5p was found to significantly decrease in H9c2 cells after OGD treatment, while it increased in the culture medium from OGD-treated H9c2 cells. Using bioinformatics databases, luciferase reporting, and western blotting assays, we identified that ERK1/2 might serve as the negative regulatory target of miR-186-5p. Combined with further transfection experiments, we indicated that miR-186-5p might inhibit the expression and activation of ERK1/2. This finding was also reflected in the reduction of their downstream cleaved caspase-3. Through functional experiments, we revealed that miR-186-5p might inhibit apoptosis and promote proliferation in OGD-treated H9c2 cells.

**Conclusions:** We demonstrated that miR-186-5p might suppress OGD-induced apoptosis in H9c2 cells by targeting the ERK1/2 pathway.

**Keywords:** miR-186-5p; ERK1/2; oxygen-glucose deprivation; H9c2; apoptosis

Submitted Apr 06, 2022. Accepted for publication Dec 02, 2022. Published online Feb 21, 2023.

doi: 10.21037/jtd-22-453

**View this article at:** <https://dx.doi.org/10.21037/jtd-22-453>

## Introduction

Acute myocardial infarction (AMI) is caused by massive myocardial ischemia and even necrosis in its branches due to sudden plaque or thrombus blocking coronary vessels (1). The process of myocardial infarction involves multiple

processes, such as apoptosis, necrosis, oxidative stress, and inflammatory response of myocardial and interstitial cells (2,3). Extensive apoptosis of cardiomyocytes causes ventricular remodeling and even heart failure, and the inhibition of cardiomyocyte apoptosis might effectively preserve cardiac function (2,3).

MicroRNAs (miRNAs) could bind to the 3'-untranslated region (3'-UTR) of the target mRNA to prevent mRNA translation and influence gene expression at the post-transcriptional level (4,5). Several studies revealed that miRNAs regulated diverse processes of cardiovascular biology, including the development of the heart, maintenance of cardiac function, and regulation of cardiomyocyte apoptosis (6-9). Our previous studies demonstrated that serum miR-186-5p levels were increased in AMI patients and might contribute to assessing the prognosis of AMI patients (10,11). However, the underlying molecular mechanism of miR-186-5p in the pathological processes of myocardial ischemia is presently unknown. In this study, we established specific models *in vivo* and *in vitro* to investigate the kinetic expression signatures of miR-186-5p. Three bioinformatics databases jointly predicted that ERK1/2 was the potential target protein of miR-186-5p. We performed various biological experiments to verify their targeting relationships and elucidate their biological effects during the process of glucose deficiency and hypoxia. We present the following article in accordance with the ARRIVE reporting checklist (available at <https://jtd.amegroups.com/article/view/10.21037/jtd-22-453/rc>).

## Methods

### Animals and AMI operation

A total of 25 specific pathogen-free/Sprague-Dawley (SD) male rats (weighing 250–300 g; 8–10 weeks old) were

purchased from the Model Animal Research Center of Jinling Hospital (MARC; China). They were later housed under regular temperature conditions and a 12 h light/dark cycle with the supplement of standard laboratory diet and water ad libitum. Experiments were performed under a project license (No. 2018GKJDWLS-03-056) granted by the Institutional Animal Care and Use Committee of Jinling Hospital in compliance with the institutional guidelines for the Care and Use of Laboratory Animals. The AMI model was induced by ligating the left anterior descending coronary artery (LAD) according to a previously described method (12). SD rats (n=25) were randomly divided into 5 groups using a table of random numbers: the AMI 2 h group (n=5), AMI 4 h group (n=5), AMI 8 h group (n=5), AMI 24 h group (n=5), and the sham-operated group (n=5). The AMI group was treated with descending coronary artery ligation, and the sham-operated group was treated with the same experimental open-chest surgery but without the LAD coronary artery ligation. To confirm that the LAD coronary artery in rats has been successfully ligated, we conducted ECG monitoring during the operation of the AMI model group. When leads II, III, etc., showed the characteristic ST-segment elevation, indicating the presence of myocardial ischemia. To further compare the changes in cardiac structure and histopathology in rats after the experimental operation, the rats were euthanized via anesthesia with 3% pentobarbital at 2, 4, 8, and 24 h after ligation, and the abdominal vein blood and ischemic myocardial tissue samples were taken for further detection. Successful surgery was also determined by observing the status of myocardial tissues after hematoxylin and eosin (H&E) staining (Figure S1).

### Highlight box

#### Key findings

- MicroRNA-186-5p may suppress oxygen-glucose deprivation-induced apoptosis in H9c2 cells by targeting the ERK1/2 pathway.

#### What is known and what is new?

- It has been reported that serum MicroRNA-186-5p levels were increased in acute myocardial infarction patients and might contribute to assessing their prognosis.
- ERK1/2 may serve as the negative regulatory target of microRNA-186-5p. MicroRNA-186-5p may inhibit the expression and activation of ERK1/2 and suppress apoptosis in oxygen-glucose deprivation-treated H9c2 cells.

#### What is the implication, and what should change now?

- The present study suggests that miR-186-5p may be used as a protective factor during acute myocardial ischemia and provides a new theoretical basis for the treatment of this disease.

### Cell culture and OGD establishment

H9c2 cells and 293T cells (Chinese Academy of Sciences, Shanghai Cell Bank, China) were cultured in a high-glucose Dulbecco's Modified Eagle's Medium (DMEM) (Gibco, USA) containing 10% Fetal Bovine Serum (FBS; Gibco) and 1% penicillin-streptomycin mixture (Gibco) at 37 °C in a humidified 5% CO<sub>2</sub> atmosphere. Oxygen-glucose deprivation (OGD) model was used to simulate the myocardial ischemic injury *in vitro*. H9c2 cells were cultured in serum-free and glucose-free DMEM medium in the AnaeroPack-Anaero bag (Mitsubishi Gas Chemical, Japan) and sealed incubator (Mitsubishi Gas Chemical) (13,14). The AnaeroPack-Anaero bag could support an environment of less than 0.1% of oxygen and more than 15% of CO<sub>2</sub>.

Four experimental groups were set up: the OGD 4 h group, OGD 8 h group, OGD 12 h group, and control group.

### Cell transfection

H9c2 cells were seeded in 6-well plates and grown to 50–60% confluence before transfection. Lipofectamine 3000 (Thermo, USA) was used to transfect the miR-186-5p mimic/mimic negative control (NC; RiboBio, China) and miR-186-5p inhibitor/inhibitor NC (RiboBio) for 24 h, following the manufacturer's instruction. The transfection concentration of mimic/mimic NC of miR-186-5p was 100 Nm, and the transfection concentration of inhibitor/inhibitor NC of miR-186-5p was 200 Nm. Then, cells were treated with OGD or not for 8 h. The effect of the synthesized mimic/inhibitor was verified by detecting the levels of miR-186-5p. The regulatory effect of miR-186-5p on the target gene was evaluated by detecting the levels of the protein produced by the target gene.

### RNA extraction, reverse transcription, and quantitative real-time polymerase chain reaction (qRT-PCR) analysis

Using TRIzol (Invitrogen, CA, USA) to extract RNA from H9c2 cells. As previously described, the phenol-chloroform purification method was applied to extract RNA from the H9c2 cells and culture medium (15). Total RNA (2  $\mu$ L) was used to synthesize complementary DNA through reverse transcription in a reaction volume of 10  $\mu$ L by an avian myeloblastosis virus (AMV) reverse transcriptase system (Takara, Japan) using TaqMan primer (Applied Biosystems, USA) set for miRNAs, as previously described (16). qRT-PCR was performed according to the protocol provided by the manufacturer of TaqMan miRNA probes (Applied Biosystems). U6 served as an internal reference for H9c2 cell samples, and MIR2911 was used for RNA extraction efficiency normalization in the cell culture medium. Relative levels of miR-186-5p were analyzed using the  $2^{-\Delta Cq}$  method.  $\Delta Cq$  was calculated by subtracting the Cq values of U6 or MIR2911 from that of miR-186-5p.

### Western blot analyses

Western blot analysis was performed to detect the expression of related proteins in rats' myocardial tissues and H9c2 cells. Total protein was extracted according to the instructions provided with protein extraction reagent (Invent, China) and RIPA lysis buffer (Beyotime, China), and quantitative analysis was

conducted using a Bradford kit (Beyotime). The protein sample was electrophoresed through SDS-PAGE (5% stacking gel and 10% resolving gel) and transferred onto polyvinylidene fluoride (PVDF) membranes (Bio-Rad, America), and subsequently blocked by 5% nonfat milk dissolved in Tris Buffered Saline with Tween 20 (TBST) for 2 h. After primary antibodies against ERK1/2 (1:1,000; CST, USA), p-ERK1/2 (1:1,000; CST), Cleaved caspase-3 (1:1,000; CST), GAPDH (1:1,000; CST) at 4 °C overnight, membranes were washed and incubated with the appropriate secondary horseradish peroxidase-labeled (HRP) antibody at room temperature for 1 h (1:5,000; Santa Cruz, America). GAPDH was used as an internal control. The bands were detected by an ECL kit (Beyotime, China), and band intensity was quantified by Image-J software.

### Luciferase reporter assay

Luciferase reporter assay was performed to identify whether *ERK1/2* was a target gene of miR-186-5p. The Pmir-REPORT (GenScript, China) plasmid (Figure S2) containing wild-type or mutated binding sites of *ERK1/2* 3'-UTR fragments (Table S1). The  $\beta$ -galactosidase ( $\beta$ -gal) reporter gene plasmid (Figure S3) was used as the internal control. The 293T cells were seeded into 24-well plates for 24 h. Then, we used lipo-2000 to co-transfected the miR-186-5p mimic/mimic NC/inhibitor/inhibitor NC, *ERK1/2* wild-type (WT)/mutator (MUT) plasmid and  $\beta$ -gal plasmid. After 48 h, the luciferase activities were analyzed using the dual-luciferase kit (Promega, America) according to the manufacturer's protocol. Relative Luciferase activity was the firefly/ $\beta$ -gal luciferase activity ratio.

### Apoptosis test

H9c2 cells were seeded into 6-well plates treated with OGD for 8 h. Subsequently, we changed the complete medium and transfected it with miR-186-6p mimic/mimic NC/inhibitor/inhibitor NC for 12 h. Eight groups were set up: the miR-186-5p mimic group; miR-186-5p mimic NC group; MiR-186-5p inhibitor group; miR-186-5p inhibitor NC group; OGD 8 h and miR-186-5p mimic group; OGD 8 h and miR-186-5p mimic NC group; OGD 8 h and miR-186-5p inhibitor group; and OGD 8 h and miR-186-5p inhibitor NC group. Annexin V-FITC/PI kit (Beyotime, China) combined with flow cytometry was used to assess cell apoptosis according to the manufacturer's instructions. A total of 10,000 cells per group were counted to assess the number of positively-stained cells.

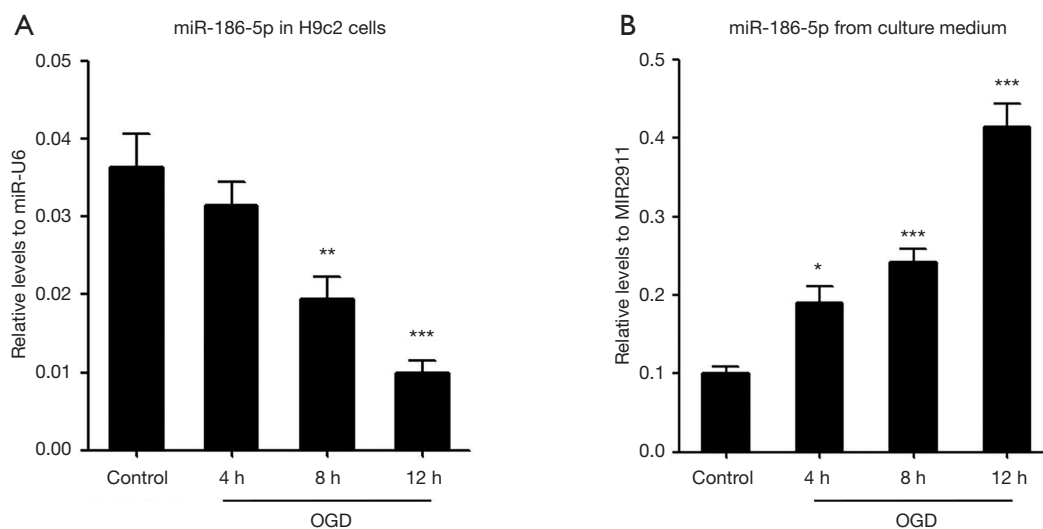


**Figure 1** Expression of miR-186-5p in H9c2 cells and culture medium after OGD treatment. (A) The relative levels of miR-186-5p in H9c2 cells after OGD treatment at 4, 8, and 12 h. (B) The relative levels of miR-186-5p in culture medium after OGD treatment at 4, 8, and 12 h. The OGD-untreated group served as the control group. \*,  $P < 0.05$ , \*\*,  $P < 0.01$ , \*\*\*,  $P < 0.001$  vs. the control group. OGD, oxygen-glucose deprivation.

### Cell counting kit-8 (CCK-8) assay

The CCK-8 kit (DOJINDO, Japan) was used to detect the regulatory effect of miR-186-5p on the proliferation of H9c2 cells after OGD treatment. The experiment was conducted according to the manufacturer's protocol.

### Statistical analyses

Data in this study are expressed as the mean  $\pm$  standard deviation of values from at least 3 independent experiments conducted in triplicate. Statistical analyses were performed using SPSS 19.0 (IBM Corp, Armonk, NY, USA). The independent samples *t* test was used to compare results between 2 groups. One-way analysis of variance (ANOVA) with Tukey's post hoc analysis was used to compare data from more than 2 groups. *P* values  $< 0.05$  were considered statistically significant.

## Results

### Expression of miR-186-5p in the OGD models

Our previous study demonstrated the different expression patterns of miR-186-5p in the serum and myocardial tissues of AMI rats (11). In the present study, we further constructed an OGD model of H9c2 cells. Through an

optical microscope to observe the cellular morphology of H9c2 cells, we confirmed that the OGD model was constructed successfully (Figure S4). qRT-PCR was used to detect the miR-186-5p expression in H9c2 cells and the culture medium after OGD treatment. The miR-186-5p levels were decreased in OGD-treated H9c2 cells at 8 and 12 h. Conversely, the levels of miR-186-5p in the cell medium were found to be significantly increased in a time-dependent manner at 4, 8, and 12 h (Figure 1). Therefore, we preliminarily speculated that miR-186-5p could be passively released from dead cells induced by OGD treatment.

### MiR-186-5p targets the 3'UTR of ERK1/2

To further explore the downstream mechanisms of miR-186-5p, 3 bioinformatics databases, including miRanda, PicTar, and TargetScan, were used to predict the possible target genes of miR-186-5p. Additionally, relevant literature was also reviewed. MiR-186-5p might bind to the 3'-UTR of ERK1/2 mRNA (Figure S5).

A luciferase reporter gene assay showed that the luciferase activity of WT-ERK1/2 3'-UTR was significantly decreased after the overexpression of miR-186-5p. In contrast, the luciferase activity of WT-TET2 3'-UTR was found to be significantly increased after the inhibition

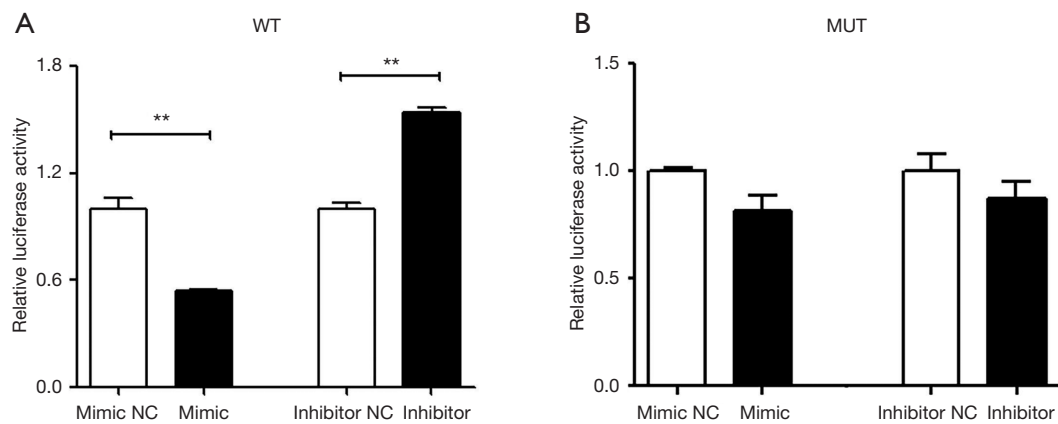


**Figure 2** Luciferase reporter gene assays to confirm ERK1/2 as a target of miR-186-5p. (A) The relative luciferase activity in 293T cells after transfecting ERK1/2-WT plasmid. (B) The relative luciferase activity in 293T cells after transfecting ERK1/2-MUT plasmid. The  $\beta$ -gal reporter gene plasmid was used as the internal reference. \*\*,  $P < 0.01$  vs. the mimic NC group. WT, wild-type; NC, negative control; MUT, mutator.

of miR-186-5p, while no difference was found in MUT-ERK1/2 3'-UTR (Figure 2). The above results indicated that miR-186-5p might specifically bind to the 3'-UTR of ERK1/2 mRNA and inhibit the expression of ERK1/2.

#### **Expression of target and apoptotic protein in the AMI and OGD models**

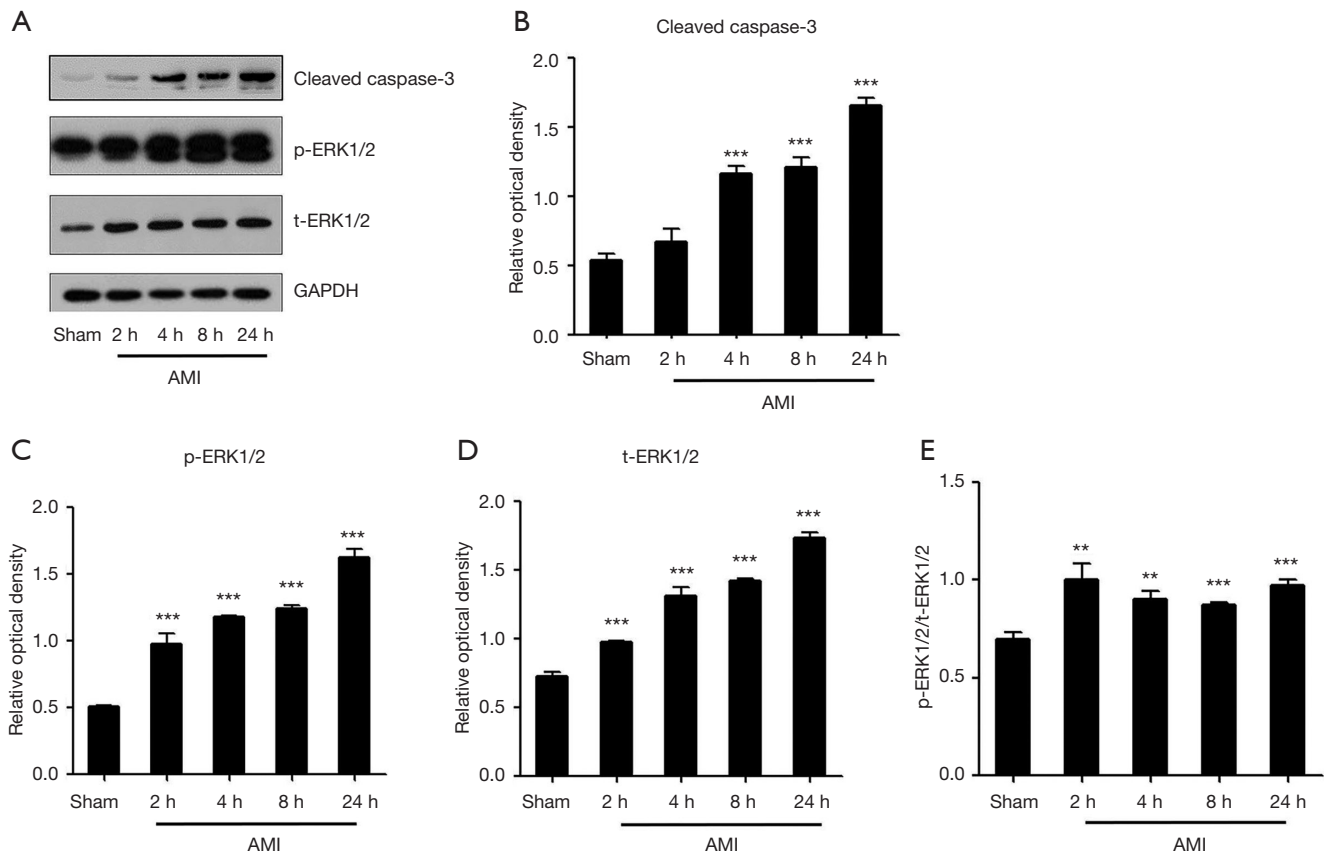
Apoptotic and target protein levels in myocardial tissues of AMI rats were determined by Western blot analyses (Figure 3). Grayscale analyses showed that the level of cleaved caspase-3 was significantly upregulated in myocardial tissues of AMI rats in a time-dependent manner at 4, 8, and 24 h. The target protein t-ERK1/2 and its phosphorylated counterpart p-ERK1/2 were significantly upregulated in myocardial tissues of AMI rats, and the ratio of p-ERK1/2/t-ERK1/2 was also significantly increased, which indicated the activation of the ERK1/2 pathway. We next extracted proteins from different phases of OGD treatment in H9c2 cells for Western blot analyses, respectively. Grayscale analyses showed that OGD treatment promoted the cleaved caspase-3 expression in a time-dependent manner. Additionally, t-ERK1/2 and p-ERK1/2 levels in OGD-treated H9c2 cells were significantly upregulated at 8 and 12 h, respectively, and the ratio of p-ERK1/2/t-ERK1/2 was also significantly increased. The above data indicated the increased apoptosis and activation of the ERK1/2 pathway after AMI and OGD treatment (Figure 4).

#### **Expression of target proteins and apoptosis protein after the overexpression or inhibition of miR-186-5p**

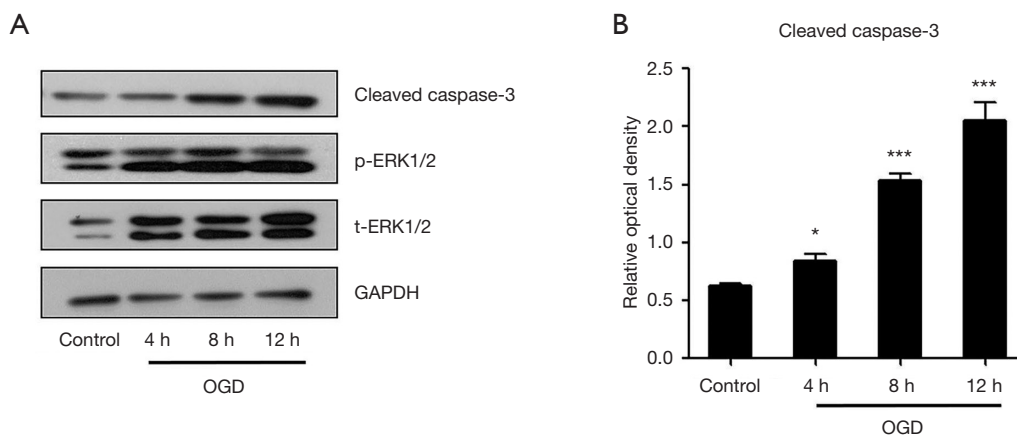
For further study, we transfected the H9c2 cells with the miR-186-5p mimic/NC and miR-186-5p inhibitor/NC. qRT-PCR results indicated that the miR-186-5p mimic significantly increased the expression of miR-186-5p (Figure 5A). Western blot analyses showed that the miR-186-5p mimic could down-regulated the expression of p-ERK1/2 and t-ERK1/2, and the ratio of p-ERK1/2/t-ERK1/2 (Figure 5B-5E). Conversely, the miR-186-5p inhibitor significantly decreased the expression of miR-186-5p (Figure 6A) and could upregulate the expression of p-ERK1/2 and t-ERK1/2, and the ratio of p-ERK1/2/t-ERK1/2 (Figure 6B-6E). Furthermore, the expression of cleaved caspase-3 was found to be decreased in the miR-186-5p mimic group (Figure 7A, 7B) but increased in the miR-186-5p inhibitor group (Figure 7C, 7D), regardless of whether OGD treatment was performed.

#### **MiR-186-5p inhibited the apoptosis of H9c2 cells in the OGD model**

To confirm the effect of miR-186-5p on the apoptosis of H9c2 cells induced by OGD treatment, we performed FCM assays to detect the apoptosis of H9c2 cells after the overexpression and inhibition of miR-186-5p (Figure 8). Compared to mimic/inhibitor NC group, the number of



**Figure 3** Expression of target and apoptotic proteins in myocardial tissues of the AMI rats. (A) Western blot analyses of apoptotic, target proteins, and GAPDH in myocardial tissues of AMI rats and sham-operated rats,  $n=5$  per group. (B-D) Grayscale analyses for the levels of cleaved caspase-3, p-ERK1/2, and t-ERK1/2 in myocardial tissues. (E) The p-ERK1/2/t-ERK1/2 ratio in myocardial tissues. GAPDH was used as the internal reference. \*\*,  $P<0.01$ , \*\*\*,  $P<0.001$  vs. the sham group. AMI, acute myocardial infarction; GAPDH, glyceraldehyde-phosphate dehydrogenase.



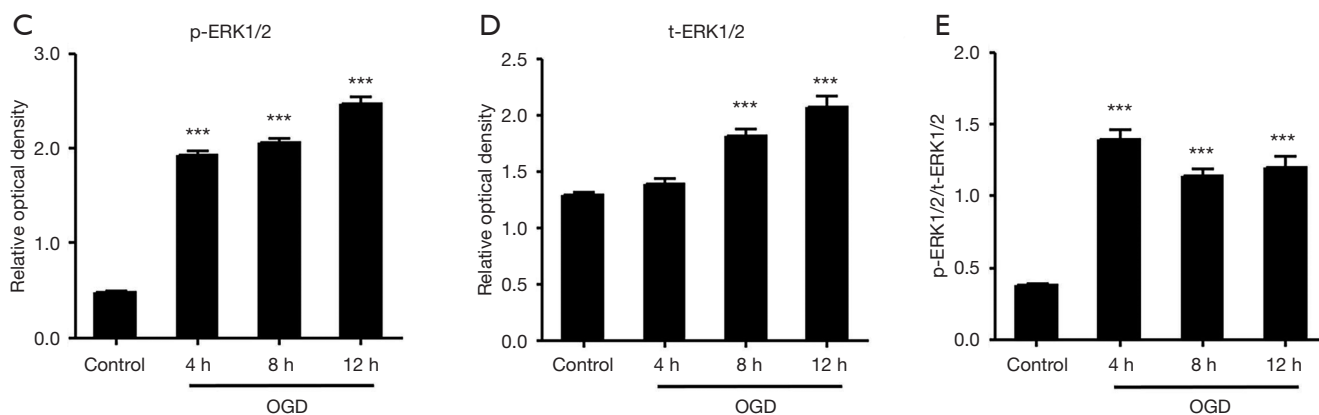


**Figure 4** Expression of target and apoptotic proteins in OGD cells. (A) Western blot analyses of apoptotic, target proteins, and GAPDH in H9c2 cells after OGD treatment at 4, 8, and 12 h. (B-D) Grayscale analyses for the levels of cleaved caspase-3, p-ERK1/2, and t-ERK1/2 in H9c2 cells after OGD treatment at 4, 8, and 12 h. (E) The p-ERK1/2/t-ERK1/2 ratio in H9c2 cells after OGD treatment at 4, 8, and 12 h. The OGD-untreated group served as the control group. GAPDH was used as the internal reference. \*\*,  $P < 0.01$ , \*\*\*,  $P < 0.001$  vs. the control group. OGD, oxygen-glucose deprivation; GAPDH, glyceraldehyde-phosphate dehydrogenase.

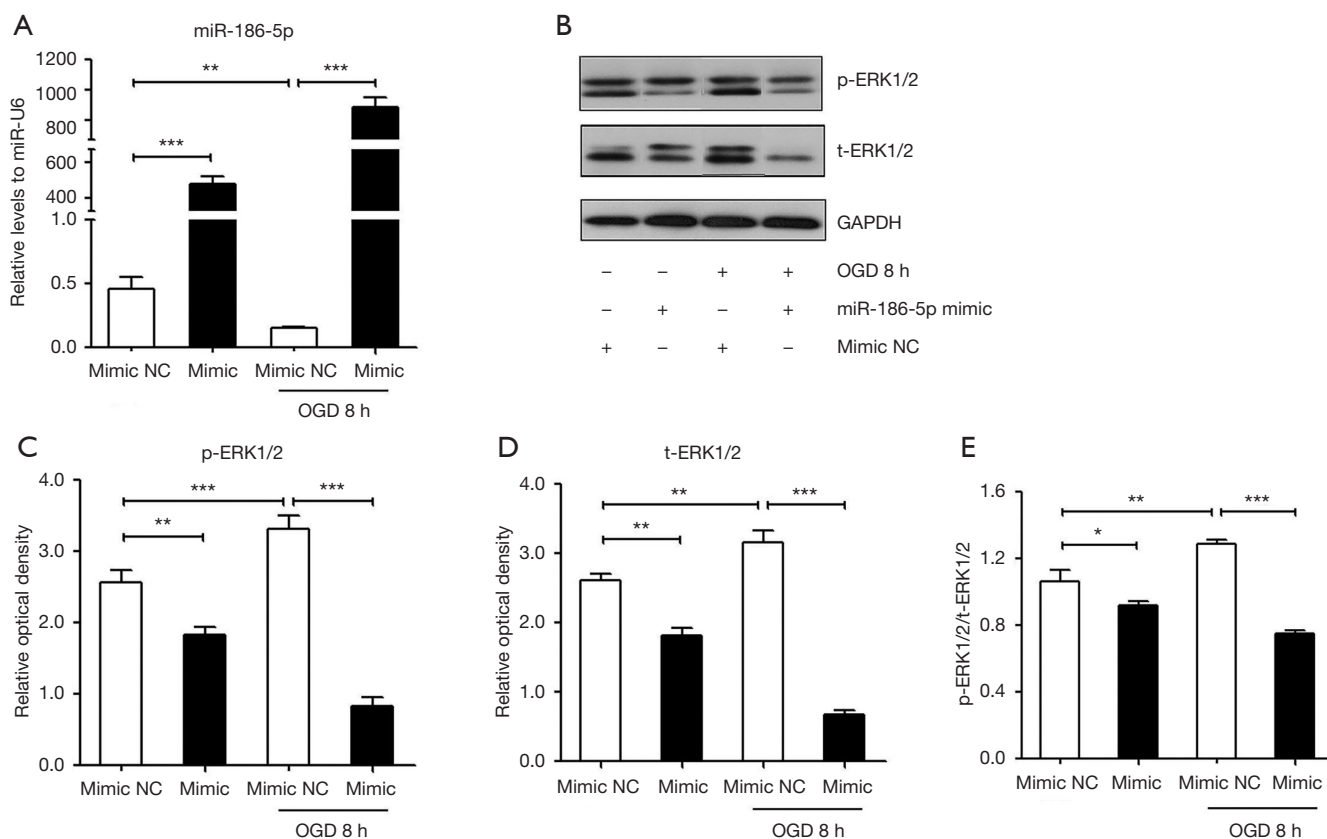


**Figure 5** Expression of the target proteins after the overexpression of miR-186-5p. (A) The relative levels of miR-186-5p in OGD-treated and untreated H9c2 cells after transfecting miR-186-5p mimic/NC. (B) Western blot analyses of the target proteins and GAPDH in OGD-treated and untreated H9c2 cells after transfecting miR-186-5p mimic/NC. (C-E) Grayscale analyses for the levels of p-ERK1/2 and t-ERK1/2 in OGD-treated and untreated H9c2 cells after transfecting miR-186-5p mimic/NC. GAPDH was used as the internal reference. \*,  $P < 0.05$ , \*\*,  $P < 0.01$ , \*\*\*,  $P < 0.001$  vs. the mimic NC group. NC, negative control; OGD, oxygen-glucose deprivation; GAPDH, glyceraldehyde-phosphate dehydrogenase.

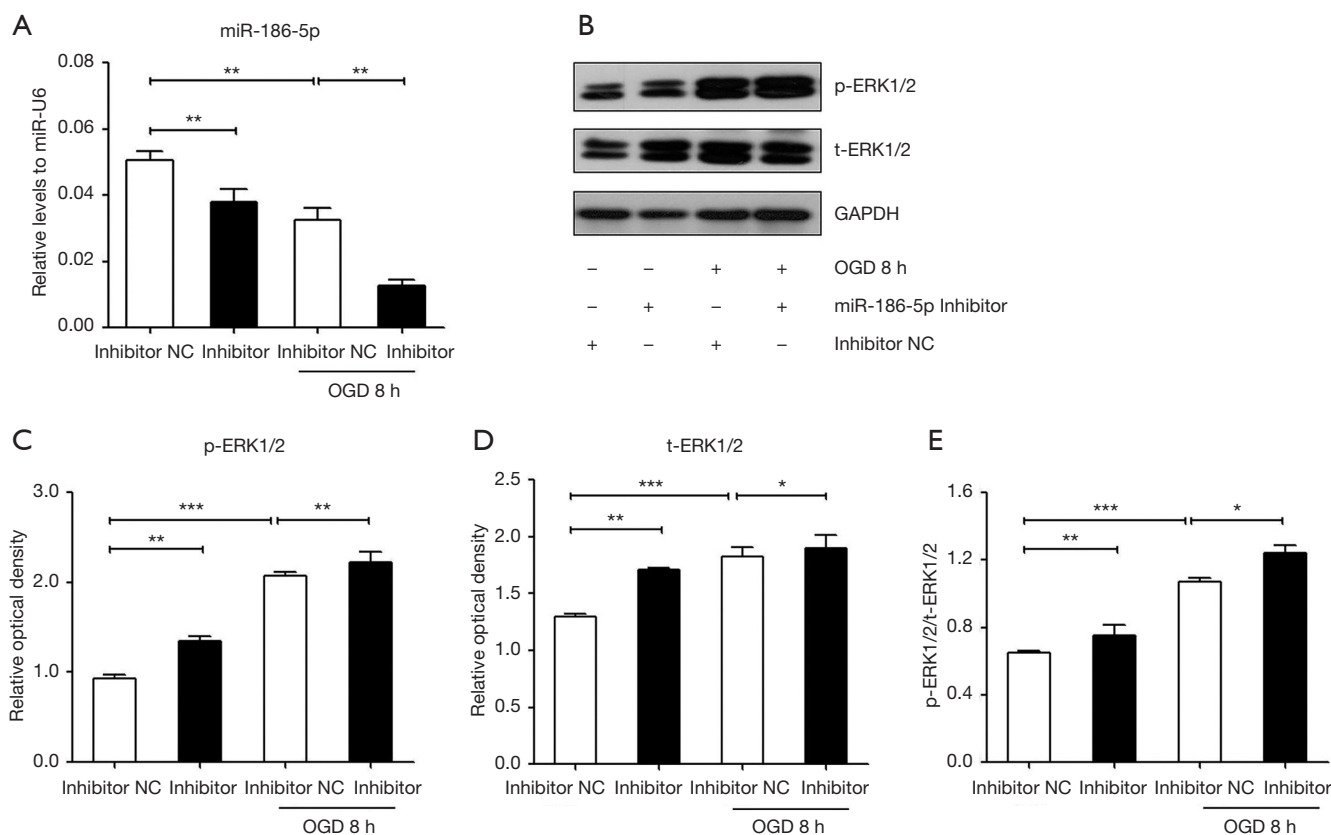


**Figure 6** Expression of the target proteins after the inhibition of miR-186-5p. (A) The relative levels of miR-186-5p in OGD-treated and untreated H9c2 cells after transfecting miR-186-5p inhibitor/NC. (B) Western blot analyses of the target proteins and GAPDH in OGD-treated and untreated H9c2 cells after transfecting miR-186-5p inhibitor/NC. (C-E) Grayscale analyses for the levels of p-ERK1/2 and t-ERK1/2 in OGD-treated and untreated H9c2 cells after transfecting miR-186-5p inhibitor/NC. GAPDH was used as the internal reference. \*,  $P < 0.05$ , \*\*,  $P < 0.01$ , \*\*\*,  $P < 0.001$  vs. the inhibitor NC group. NC, negative control; OGD, oxygen-glucose deprivation; GAPDH, glyceraldehyde-phosphate dehydrogenase.

apoptotic cells was significantly decreased in the miR-186-5p mimic group, whereas opposing results were noted in the miR-186-5p inhibitor group. Furthermore, OGD treatment was found to enhance the apoptosis of H9c2 cells.

#### *MiR-186-5p promoted the proliferation of H9c2 cells in the OGD model*

To further evaluate the effects of miR-186-5p on the proliferation of H9c2 cells induced by OGD treatment, we performed the CCK-8 assays to detect the proliferation of H9c2 cells after the overexpression and inhibition of miR-186-5p (Figure 9). Consequently, the proliferation was significantly increased at 48 and 60 h in the miR-186-5p mimic group and significantly increased at 24, 36, 48, and 60 h in the OGD-treated and miR-186-5p mimic groups, respectively. Meanwhile, the proliferation of the OGD-

treated H9c2 cells was found to be significantly increased compared with that of the OGD-untreated H9c2 cells at 60 h after transfecting miR-186-5p mimic.

#### **Discussion**

In the present study, we found that the level of miR-186-5p was decreased in the OGD-treated H9c2 cells. By using bioinformatics databases analysis and luciferase reporter gene assay, we identified that ERK1/2 might serve as the negative regulatory target of miR-186-5p. Through further transfection experiments, we demonstrated that miR-186-5p might inhibit the expression and activation of ERK1/2, which was also reflected in the reduction of their downstream cleaved caspase-3. Functional experiments helped us to reveal that miR-186-5p may inhibit apoptosis and promote the proliferation of OGD-treated H9c2

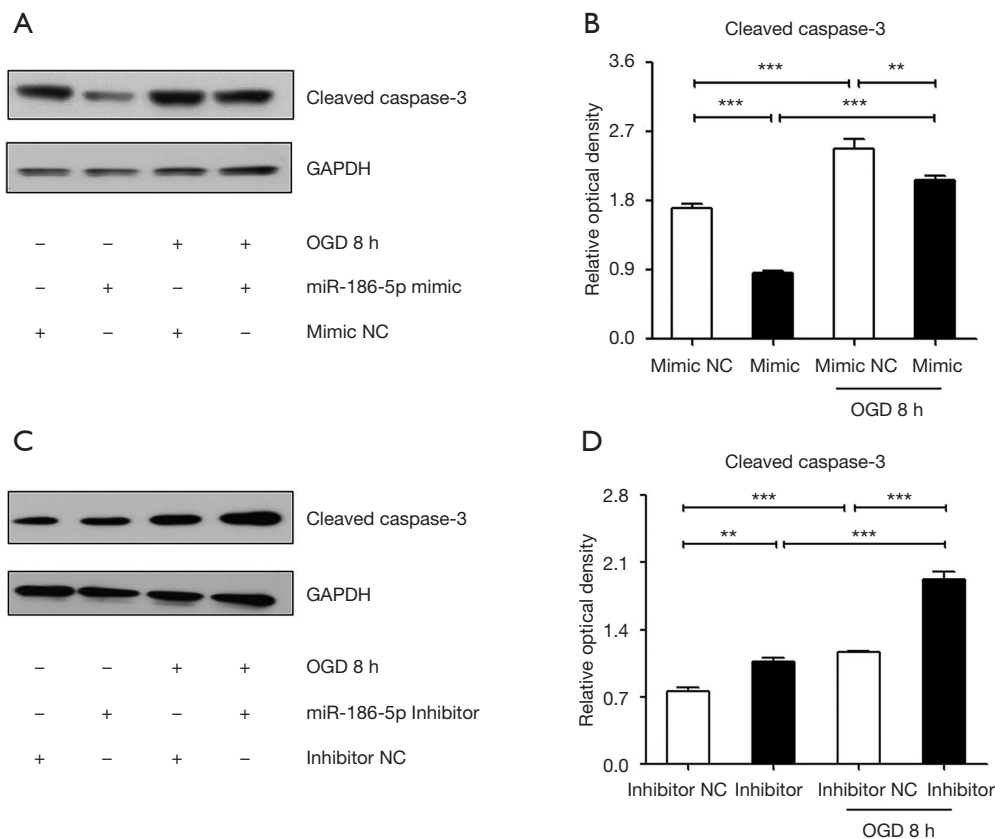


**Figure 7** Expression of apoptotic protein after the overexpression or inhibition of miR-186-5p. (A) Western blot analyses of apoptotic protein and GAPDH in OGD-treated and untreated H9c2 cells after transfecting miR-186-5p mimic/NC. (B) Grayscale analyses for the levels of cleaved caspase-3 in OGD-treated and untreated H9c2 cells after transfecting miR-186-5p mimic/NC. (C) Western blot analyses of apoptotic protein and GAPDH in OGD-treated and untreated H9c2 cells after transfecting miR-186-5p inhibitor/NC. (D) Grayscale analyses for the levels of cleaved caspase-3 in OGD-treated and untreated H9c2 cells after transfecting miR-186-5p inhibitor/NC. GAPDH was used as the internal reference. \*\*,  $P < 0.01$ , \*\*\*,  $P < 0.001$  vs. Mimic NC group. OGD, oxygen-glucose deprivation; NC, negative control; GAPDH, glyceraldehyde-phosphate dehydrogenase.

cells. Consequently, we concluded that miR-186-5p might suppress OGD-induced apoptosis in H9c2 cells by targeting the ERK1/2 pathway.

MiRNA is a new class of disease biomarkers that can be used to detect biogenesis, including transcription, processing, splicing, export to the cytoplasm, maturation, and binding to the target gene. Our previous study found that the levels of miR-186-5p were increased in the serum of AMI patients and AMI rats (10,11). In the present study, miR-186-5p expression was decreased in H9c2 cells after OGD treatment but increased in the culture medium from the OGD-treated cells. Combining with these aforementioned results, we speculated that miR-186-5p may be passively released from dead cells induced by OGD treatment.

MiRNAs pair with their target mRNA to regulate translation. In mammals, about 60% of all protein-coding genes were controlled by miRNAs (17). In the present study, bioinformatics analysis and luciferase reporter gene assay demonstrated that miR-186-5p could specifically bind to *ERK1/2* mRNA 3'-UTR. As a member of the mitogen-activated protein kinase (MAPK) family, ERK1/2 was an important serine-threonine protein kinase, which could be activated by phosphorylation to transduce cell signals to the nucleus in multiple steps. It was mainly involved in cell proliferation, differentiation, and apoptosis (18,19). The MAPK family plays an important role in inflammatory reactions in various diseases, and the ERK1/2-NF- $\kappa$ B pathway affects the activation of the NLRP3 inflammasome

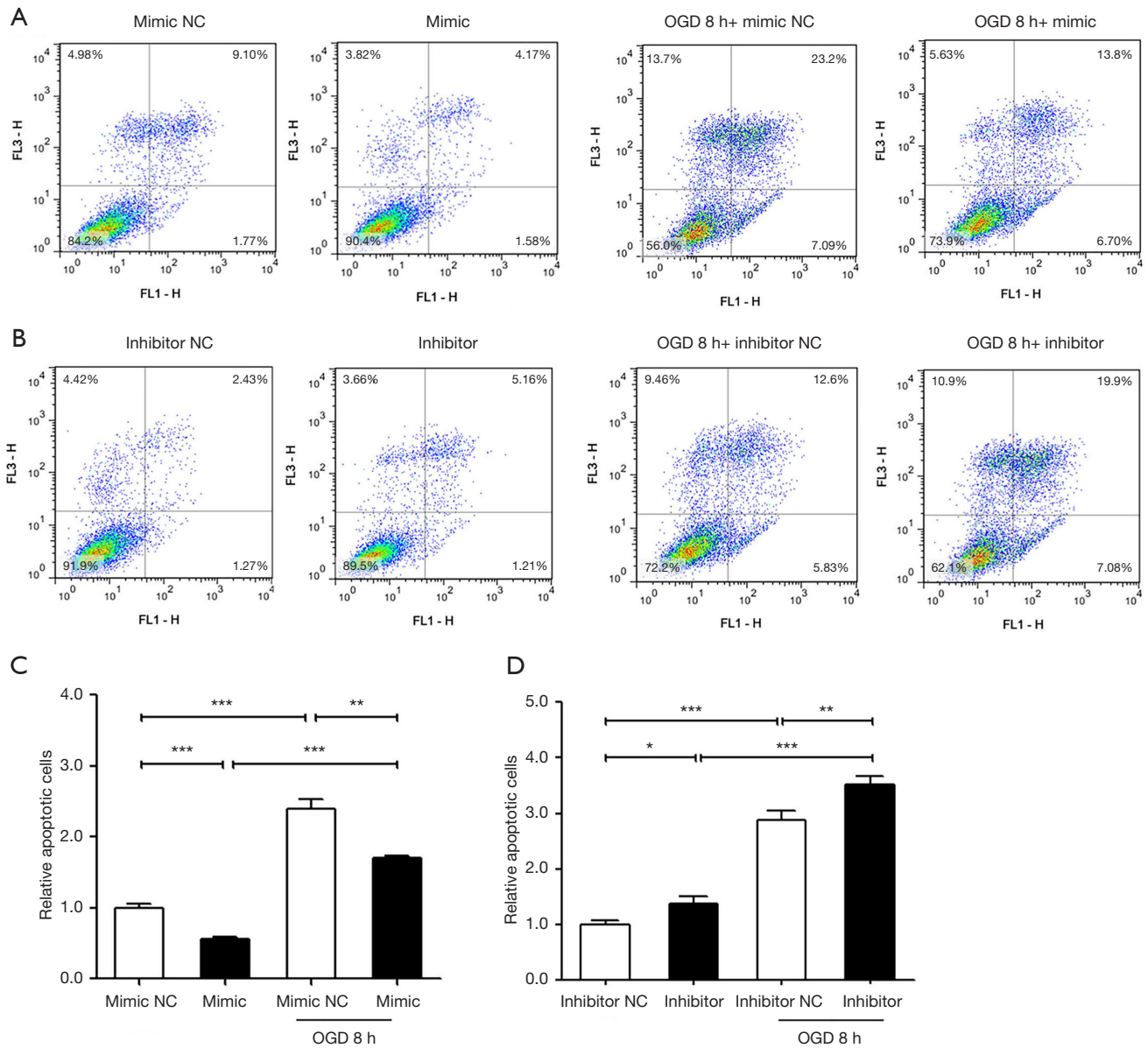


**Figure 8** Flow cytometry to analyze the H9c2 cell apoptosis. (A,C) The number of apoptotic cells in OGD-treated and untreated H9c2 cells after transfecting miR-186-5p mimic/NC. \*\*,  $P < 0.01$ , \*\*\*,  $P < 0.001$  vs. the mimic NC group. (B,D) The number of apoptotic cells in OGD-treated and untreated H9c2 cells after transfecting miR-186-5p inhibitor/NC. \*,  $P < 0.05$ , \*\*,  $P < 0.01$ , \*\*\*,  $P < 0.001$  vs. the inhibitor NC group. NC, negative control; OGD, oxygen-glucose deprivation.

in the atherosclerosis process (20). Studies have shown that ERK1/2 could affect myocardial fibrosis after infarction by regulating the proliferation of myocardial fibroblasts (21). ERK1/2 has also been shown to participate in the hyperplasia and hypertrophy of ventricular myocytes after myocardial infarction by influencing the expression of brain natriuretic peptide and c-fos (22). Additionally, inhibition

of ERK1/2 activation reduces mitochondrial lysis in H9c2 cells, thereby alleviating myocardial apoptosis induced by reoxygenation after hypoxia (23,24). Therefore, ERK1/2 plays a complex and important role in the hypoxic stress environment of cardiomyocytes.

An increasing number of studies have demonstrated that miRNAs play important roles in cardiogenesis,

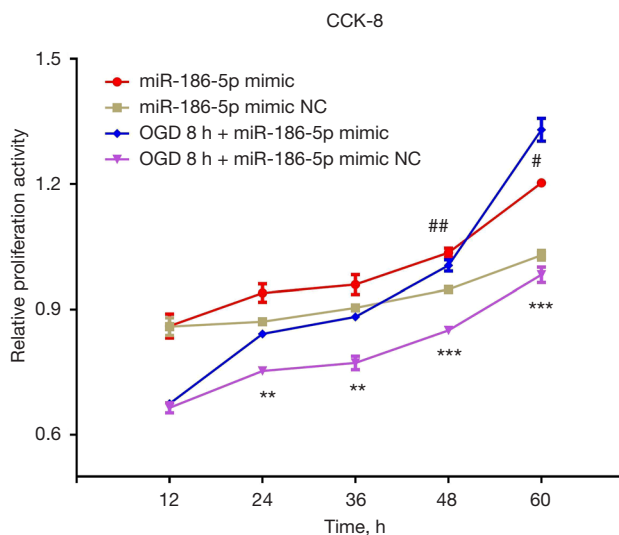


**Figure 9** CCK-8 assays to analyze the H9c2 cell proliferation. “#” symbol represented the comparison of the OGD-untreated H9c2 cells between the miR-186-5p mimic group and the mimic NC group at the corresponding time points; #,  $P < 0.05$ , ##,  $P < 0.01$ . “\*” symbol represented the comparison of the OGD-treated H9c2 cells between the miR-186-5p mimic group and the mimic NC group at the corresponding time points; \*\*,  $P < 0.01$ , \*\*\*,  $P < 0.001$ . NC, negative control; OGD, oxygen-glucose deprivation.

endothelial injury, and abnormal inflammation by the regulation of apoptosis of cardiomyocytes (25-29). In this study, transfection experiments were further performed to determine the specific role of miR-186-5p in OGD-treated H9c2 cells. Our results suggested that miR-186-5p might inhibit the expression and activation of ERK1/2. This finding was also reflected in the reduction of their downstream apoptosis-related proteins, such as cleaved caspase-3. Flow cytometry assays were performed to reveal that miR-186-5p could attenuate the OGD-induced apoptosis of H9c2 cells. Additionally, the CCK-8 experiments were conducted to clarify that miR-186-5p alleviated the reduced proliferation of H9c2 cells induced by OGD treatment. The studies have shown that miR-186-5p might regulate the proliferation, apoptosis, and inflammatory response of cardiomyocytes by targeting IGF-1 and inhibiting TLR3 (30-34). However, no reports have been found about miR-186-5p targeting ERK1/2 to induce myocardial cell injury caused by glucose deficiency and hypoxia. The present study further identified that miR-186-5p in H9c2 cells might be used as a protective factor to inhibit cell damage caused by ischemia and hypoxia.

Our study had some limitations. First, although this study confirmed the association between miR-186-5p and its target protein and the possible role of miR-186-5p in OGD-treated H9c2 cells, the mechanism of how ERK1/2 affected downstream molecules, such as the pro-caspase3 or the poly (ADP-ribose) polymerase (PARP) to regulate cell apoptosis, was still unknown. Additionally, further experiments are needed to elucidate the underlying signaling pathway and whether the altered apoptotic and proliferative capacity of cardiomyocytes was regulated exclusively by miR-186-5p and ERK1/2. To confirm the effect of miR-186-5p on myocardial ischemia and hypoxia, it is also necessary to construct animal models of overexpression or inhibition of miR-186-5p and evaluate the value of antagonistic myocardial apoptosis or therapeutic *in vivo*.

## Conclusions

The present study demonstrated that miR-186-5p might inhibit the apoptosis and promote the proliferation of H9c2 cells induced by glucose deficiency and hypoxia by targeting ERK1/2. These findings suggest that miR-186-5p can be used as a protective factor during acute myocardial ischemia. This study provides a new theoretical basis for treating this disease.

## Acknowledgments

**Funding:** This work was supported by the National Natural Science Foundation of China (Nos. 81871702; 82172360).

## Footnote

**Reporting Checklist:** The authors have completed the ARRIVE reporting checklist. Available at <https://jtd.amegroups.com/article/view/10.21037/jtd-22-453/rc>

**Data Sharing Statement:** Available at <https://jtd.amegroups.com/article/view/10.21037/jtd-22-453/dss>

**Conflicts of Interest:** All authors have completed the ICMJE uniform disclosure form (available at <https://jtd.amegroups.com/article/view/10.21037/jtd-22-453/coif>). The authors have no conflicts of interest to declare.

**Ethical Statement:** The authors are accountable for all aspects of the work in ensuring that questions related to the accuracy or integrity of any part of the work are appropriately

investigated and resolved. Experiments were performed under a project license (No. 2018GKJDWLS-03-056) granted by the Institutional Animal Care and Use Committee of Jinling Hospital in compliance with the institutional guidelines for the Care and Use of Laboratory Animals.

**Open Access Statement:** This is an Open Access article distributed in accordance with the Creative Commons Attribution-NonCommercial-NoDerivs 4.0 International License (CC BY-NC-ND 4.0), which permits the non-commercial replication and distribution of the article with the strict proviso that no changes or edits are made and the original work is properly cited (including links to both the formal publication through the relevant DOI and the license). See: <https://creativecommons.org/licenses/by-nc-nd/4.0/>.

## References

- Falk E, Nakano M, Bentzon JF, et al. Update on acute coronary syndromes: the pathologists' view. *Eur Heart J* 2013;34:719-28.
- Han Y, Cai Y, Lai X, et al. lncRNA RMRP Prevents Mitochondrial Dysfunction and Cardiomyocyte Apoptosis via the miR-1-5p/hsp70 Axis in LPS-Induced Sepsis Mice. *Inflammation* 2020;43:605-18.
- Wei L, Zhou Q, Tian H, et al. Integrin  $\beta$ 3 promotes cardiomyocyte proliferation and attenuates hypoxia-induced apoptosis via regulating the PTEN/Akt/Mtor and ERK1/2 pathways. *Int J Biol Sci* 2020;16:644-54.
- Mohr AM, Mott JL. Overview of microRNA biology. *Semin Liver Dis* 2015;35:3-11.
- Bartel DP. MicroRNAs: target recognition and regulatory functions. *Cell* 2009;136:215-33.
- Wojciechowska A, Braniewska A, Kozar-Kamińska K. MicroRNA in cardiovascular biology and disease. *Adv Clin Exp Med* 2017;26:865-74.
- Xiao X, Lu Z, Lin V, et al. MicroRNA miR-24-3p Reduces Apoptosis and Regulates Keap1-Nrf2 Pathway in Mouse Cardiomyocytes Responding to Ischemia/Reperfusion Injury. *Oxid Med Cell Longev* 2018;2018:7042105.
- Ning S, Li Z, Ji Z, et al. MicroRNA 494 suppresses hypoxia/reoxygenation induced cardiomyocyte apoptosis and autophagy via the PI3K/AKT/Mtor signaling pathway by targeting SIRT1. *Mol Med Rep* 2020;22:5231-42.
- Li AY, Yang Q, Yang K. miR-133a mediates the hypoxia-induced apoptosis by inhibiting TAGLN2 expression in cardiac myocytes. *Mol Cell Biochem* 2015;400:173-81.
- Wu J, Song J, Wang C, et al. Identification of serum microRNAs for cardiovascular risk stratification in dyslipidemia subjects. *Int J Cardiol* 2014;172:232-4.
- Li Z, Wu J, Wei W, et al. Association of Serum miR-186-5p With the Prognosis of Acute Coronary Syndrome Patients After Percutaneous Coronary Intervention. *Front Physiol* 2019;10:686.
- Yang B, Lin H, Xiao J, et al. The muscle-specific microRNA miR-1 regulates cardiac arrhythmogenic potential by targeting GJA1 and KCNJ2. *Nat Med* 2007;13:486-91.
- Katoh C, Osanai T, Tomita H, et al. Brain natriuretic peptide is released from human astrocytoma cell line U373MG under hypoxia: a possible role in anti-apoptosis. *J Endocrinol* 2011;208:51-7.
- Kamiya T, Kwon AH, Kanemaki T, et al. A simplified model of hypoxic injury in primary cultured rat hepatocytes. *In Vitro Cell Dev Biol Anim* 1998;34:131-7.
- Wang C, Wan S, Yang T, et al. Increased serum microRNAs are closely associated with the presence of microvascular complications in type 2 diabetes mellitus. *Sci Rep* 2016;6:20032.
- Lu P, Wang F, Wu J, et al. Elevated Serum miR-7, miR-9, miR-122, and miR-141 Are Noninvasive Biomarkers of Acute Pancreatitis. *Dis Markers* 2017;2017:7293459.
- Friedman RC, Farh KK, Burge CB, et al. Most mammalian mRNAs are conserved targets of microRNAs. *Genome Res* 2009;19:92-105.
- Yang SH, Sharrocks AD, Whitmarsh AJ. Transcriptional regulation by the MAP kinase signaling cascades. *Gene* 2003;320:3-21.
- Yoon S, Seger R. The extracellular signal-regulated kinase: multiple substrates regulate diverse cellular functions. *Growth Factors* 2006;24:21-44.
- Yin R, Zhu X, Wang J, et al. MicroRNA-155 promotes the ox-LDL-induced activation of NLRP3 inflammasomes via the ERK1/2 pathway in THP-1 macrophages and aggravates atherosclerosis in ApoE<sup>-/-</sup> mice. *Ann Palliat Med* 2019;8:676-89.
- Liu Z, Xu Q, Yang Q, et al. Vascular peroxidase 1 is a novel regulator of cardiac fibrosis after myocardial infarction. *Redox Biol* 2019;22:101151.
- He Q, Harding P, LaPointe MC. PKA, Rap1, ERK1/2, and p90RSK mediate PGE2 and EP4 signaling in neonatal ventricular myocytes. *Am J Physiol Heart Circ Physiol* 2010;298:H136-43.
- Zhao L, Zhuang J, Wang Y, et al. Propofol Ameliorates H9c2 Cells Apoptosis Induced by Oxygen Glucose Deprivation and Reperfusion Injury via Inhibiting High

- Levels of Mitochondrial Fusion and Fission. *Front Pharmacol* 2019;10:61.
24. Li F, Li D, Tang S, et al. Quercetin Protects H9c2 Cardiomyocytes against Oxygen-Glucose Deprivation/Reoxygenation-Induced Oxidative Stress and Mitochondrial Apoptosis by Regulating the ERK1/2/DRP1 Signaling Pathway. *Evid Based Complement Alternat Med* 2021;2021:7522175.
  25. Kaur A, Mackin ST, Schlosser K, et al. Systematic review of microRNA biomarkers in acute coronary syndrome and stable coronary artery disease. *Cardiovasc Res* 2020;116:1113-24.
  26. Wu S, Sun H, Sun B. MicroRNA-145 is involved in endothelial cell dysfunction and acts as a promising biomarker of acute coronary syndrome. *Eur J Med Res* 2020;25:2.
  27. Wang X, Shang Y, Dai S, et al. MicroRNA-16-5p Aggravates Myocardial Infarction Injury by Targeting the Expression of Insulin Receptor Substrates 1 and Mediating Myocardial Apoptosis and Angiogenesis. *Curr Neurovasc Res* 2020;17:11-7.
  28. Zhao Z, Du S, Shen S, et al. microRNA-132 inhibits cardiomyocyte apoptosis and myocardial remodeling in myocardial infarction by targeting IL-1 $\beta$ . *J Cell Physiol* 2020;235:2710-21.
  29. Yang B, Dong R, Zhao H. Inhibition of microRNA-346 inhibits myocardial inflammation and apoptosis after myocardial infarction via targeting NFIB. *Eur Rev Med Pharmacol Sci* 2020;24:11752-60.
  30. Jiang J, Mo H, Liu C, et al. Inhibition of miR-186-5p contributes to high glucose-induced injury in AC16 cardiomyocytes. *Exp Ther Med* 2018;15:627-32.
  31. Xu H, Li J, Zhao Y, et al. TNF $\alpha$ -induced downregulation of microRNA-186 contributes to apoptosis in rat primary cardiomyocytes. *Immunobiology* 2017;222:778-84.
  32. Liu Y, Zheng W, Pan Y, et al. Low expression of miR-186-5p regulates cell apoptosis by targeting toll-like receptor 3 in high glucose-induced cardiomyocytes. *J Cell Biochem* 2019;120:9532-8.
  33. Wang R, Bao H, Zhang S, et al. miR-186-5p Promotes Apoptosis by Targeting IGF-1 in SH-SY5Y OGD/R Model. *Int J Biol Sci* 2018;14:1791-9.
  34. Yao Y, Zhang X, Chen HP, et al. MicroRNA-186 promotes macrophage lipid accumulation and secretion of pro-inflammatory cytokines by targeting cystathionine  $\gamma$ -lyase in THP-1 macrophages. *Atherosclerosis* 2016;250:122-32.
- (English Language Editor: C. Mullens)

**Cite this article as:** Nie W, Wu J, Yu X, Li Z, Cai X, Wei W, Wang C, Wang J. MicroRNA-186-5p inhibits H9c2 cells apoptosis induced by oxygen-glucose deprivation by targeting ERK1/2. *J Thorac Dis* 2023;15(2):529-541. doi: 10.21037/jtd-22-453

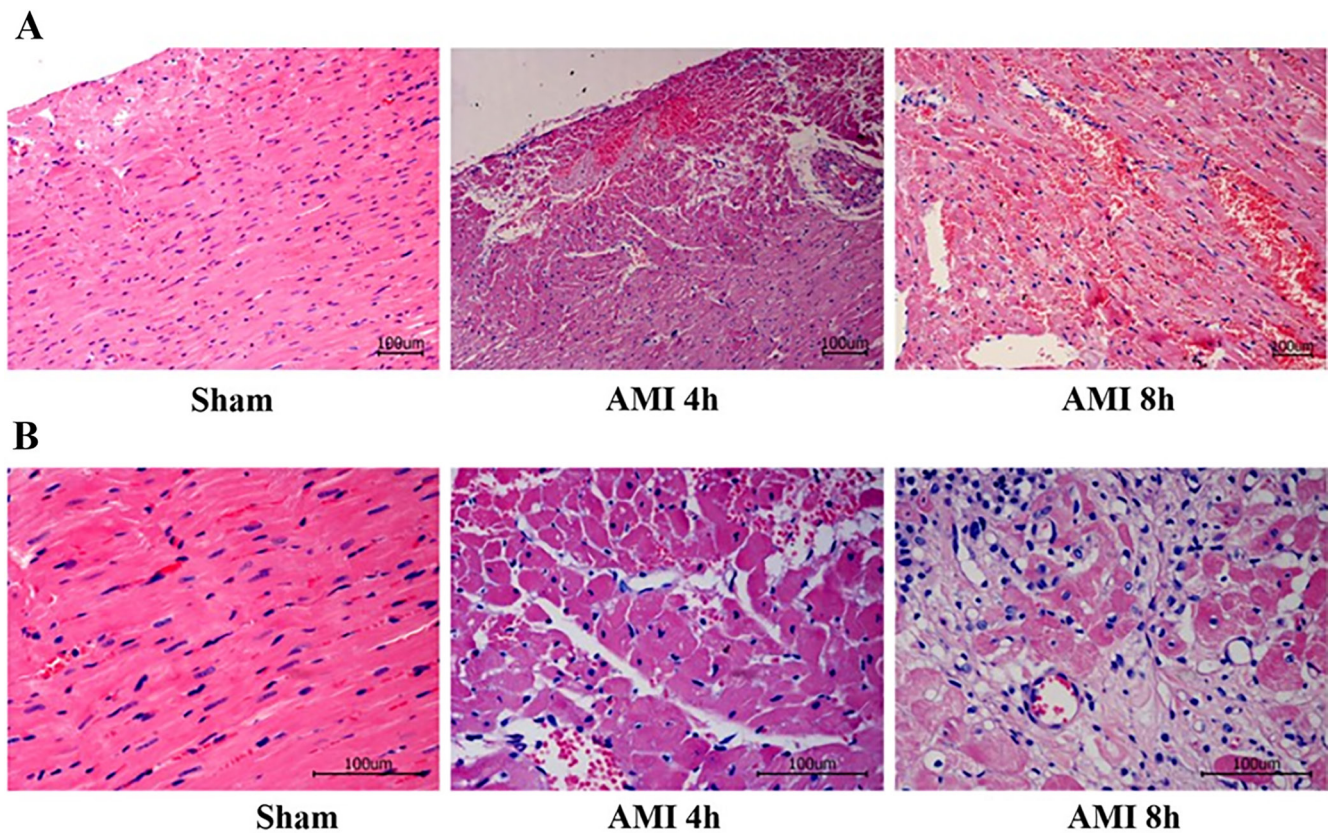


**Figure S1** Myocardial tissues of rats stained with H&E. The myocardial tissues of rats in each group were stained with H&E. In the sham-operated group, the myocardial cells were arranged neatly, and the nucleus was clearly visible, and the cell membrane was intact, and only a few inflammatory cells could be observed. While, in the AMI model group, the cross-sectional myocardial tissues of the infarct regions showed the characteristics of necrosis and inflammatory infiltration, manifested as its structural disorder, interstitial enlargement, visible vacuoles in the cytoplasm, pyknotic and hyperchromatic nuclei, hyperemia, and leukocyte infiltration. And with the longer ligation time, the above changes are more obvious. The results of H&E staining indicated that the LAD coronary ligation surgery had successfully resulted in myocardial ischemia and infarction (A:  $\times 100$ ; B:  $\times 400$ ). H&E, hematoxylin and eosin; AMI, acute myocardial infarction; LAD, left anterior descending coronary artery.

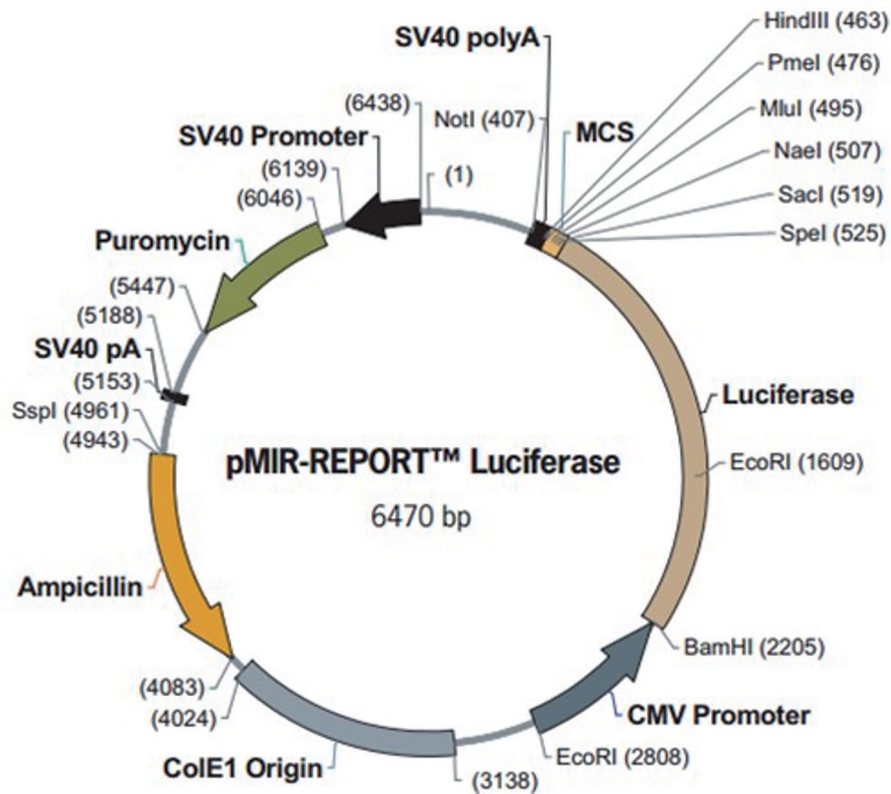


**Figure S2** Schematic diagram of the plasmid containing the pMIR-report luciferase reporter gene.

**Table S1** Sequences of the primers used for the ERK1/2 luciferase reporter assay

Gene	Sequence (5'-3')
<i>ERK1/2-WT</i>	TTTCACCTTAATTCTTTGATGTTGTA
<i>ERK1/2-MUT</i>	TTTCACCTTATAAGAAATGATGTTGTA

For the WT sequence, the part in bold is the complementary binding site of miR-186-5p with the target gene, and the part in bold for the MUT sequence is the mutation site.

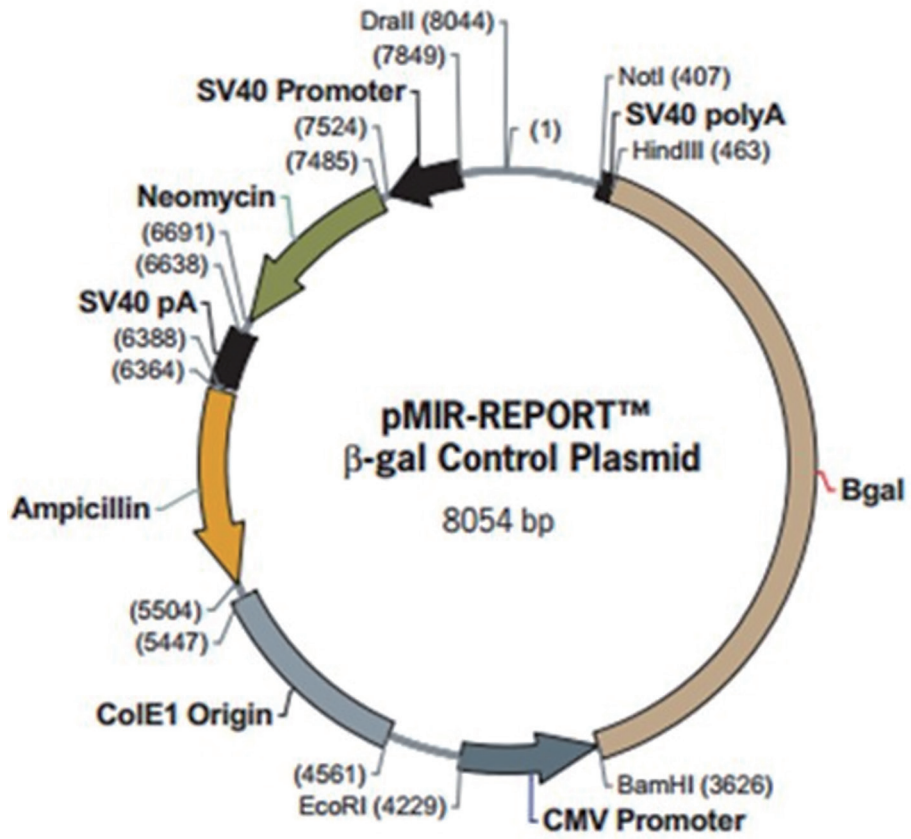
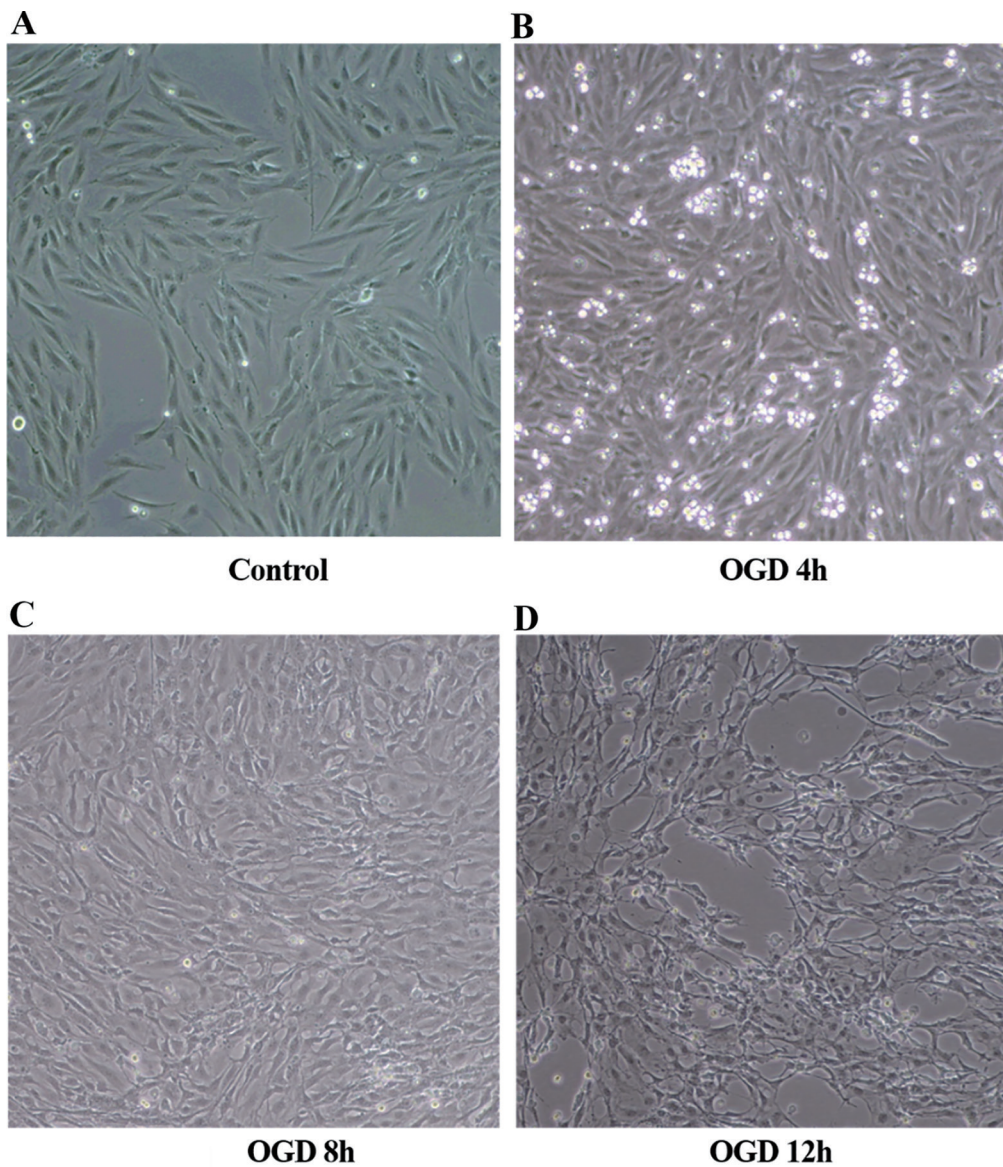


Figure S3 Schematic diagram of the β-gal reporter plasmid.



**Figure S4** H9c2 cells under a light microscope ( $\times 100$ ). We observed the H9C2 cells and found that the cells in the Control group were fusiform with regular morphology and well-adhered to the wall. Besides, they had a clear nucleus and abundant cytoplasm. Conversely, some of the OGD-treated H9C2 cells were detached from the culture plate, and they were shriveled and branched. These cells also showed fragmentation of the nucleus, reduction of the cytoplasm, and a reduced refractive activity; the changes were more pronounced with an increase in the duration of the OGD treatment. OGD, oxygen-glucose deprivation.

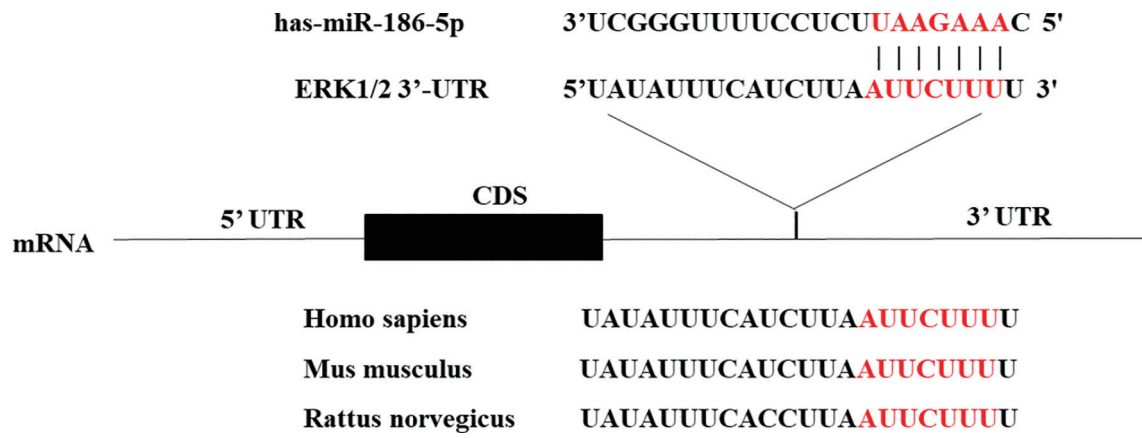


Figure S5 Binding sites of miR-186-5p and the ERK1/2 3'-UTR region.